The Adiabatic-to-Diabatic Transformation Angle and the Berry Phase for Coupled Jahn–Teller/Renner–Teller Systems: The F + H_2 as a Case Study

Anita Das,[a] Debasis Mukhopadhyay,[a]# Satrajit Adhikari,[b] and Michael Baer*[c]

The approach to calculate improved, two-state, adiabatic-to-diabatic transformation angles (also known as mixing angles), presented before (see Das et al., J Chem Phys 2010, 133, 084107), was used here while studying the F + H_2 system. However, this study is characterized by two new features: (a) it is the first of its kind in which is studied the interplay between Renner–Teller (RT) and Jahn–Teller (JT) nonadiabatic coupling terms (NACT); (b) it is the first of its kind in which is reported the effect of an upper singular RT-NACT on a lower two-state (JT) mixing angle. The fact that the upper NACT is singular (it is shown to be a quasi-Dirac δ-function) enables a semi-analytical solution for this perturbed mixing angle. The present treatment, performed for the F + H_2 system, revealed the existence of a novel parameter, η, the Jahn–Renner coupling parameter (JRCP), which yields, in an unambiguous way, the right intensity of the RT coupling (as resembled, in this case, by the quasi-Dirac δ-function) responsible for the fact that the final end-of-the contour angle (identified with the Berry phase) is properly quantized. This study implies that the numerical value of this parameter is a pure number (independent of the molecular system): $\eta = 2\sqrt{2}/\pi$ (= 0.9003) and that there is a good possibility that this value is a novel characteristic molecular constant for a certain class of tri-atomic systems. © 2011 Wiley Periodicals, Inc.

DOI: 10.1002/qua.23272

Introduction

As is well-known, the literature contains numerous studies on the adiabatic-to-diabatic transformation (ADT) angle (also known as the mixing angle) related to many different systems. In general, these studies are divided into two categories: (a) one category contains studies related to ADT angles, which have their origin in the Jahn–Teller (JT) conical intersections (CIs) such as H_2 + H,[1–3] C_2H,[4] H_2O,[5] H_2N,[6] C_2H_2,[7] NO_2,[8] CH_3NH_2,[9] C_5H_4NH,[10] H_2 + H^+,[11] etc.; (b) the second category contains studies related to ADT angles, which have their origin in the Renner–Teller (RT) CIs such as H_2N,[12] $C_2H_2^+$,[13] H_2CN,[14] etc. This partitioning is somewhat artificial because molecular systems have both types of CIs. Therefore, the kind of numerical treatment to be performed depends first and most on the type of state to be considered (and to a lesser extent, also, on the corresponding configuration space). Thus, if the state is a Σ-state, we usually expect it to form, with its nearest state, a JT CI but if it is a Π-state then it most likely forms with that state (which is also a Π-state) a RT CI etc.

The experience we had so far is that the two types of CIs are independent, namely, while calculating the ADT angles (along given contours) the two calculations can be performed independently. This belief prevailed until recently, when, as studying the title system, we encountered difficulties with the issue known as the quantization[15,16] of the Berry phase[17] which did not converge to the correct limit (see discussion in Ref. [18]). These difficulties are elaborated below.

Comment

We just remind the reader that the quantization of the two-state end-of-the-contour ADT angle, Γ (which is identified as the Berry phase) is an integer multiple of π (or zero).[17] Satisfying this demand in a given region is the only way to guarantee that the resulting diabatic potential energy surfaces (PESs) are single-valued in that region of configuration space (see Appendix A).

Theory

The three-state model

Our goal is to calculate well-behaved diabatic PESs for a tri-atomic system (in this case F + H_2), and to do that we consider a plane that contains three atoms (A, B, and C) where a point in configuration space is described in terms of three (Cartesian) coordinates (r, R, and θ). Here, r is the distance between two atoms (usually the atoms that form the diatomic molecule, BC), R is a distance between the third atom, A, and

[a] A. Das, D. Mukhopadhyay
Department of Chemistry, University of Calcutta, Kolkata 700 009, India
[b] S. Adhikari
Department of Physical Chemistry, Indian Association for Cultivation of Science, Jadavpur, Kolkata 700 032, India
[c] M. Baer
The Fritz Haber Research Center for Molecular Dynamics, The Hebrew University of Jerusalem, Jerusalem 91904, Israel
*E-mail: michaelb@fh.huji.ac.il
#Corresponding author; e-mail: dm.chem.cu@gmail.com

Contract grant sponsor: BRNS, India; contract grant number: 2009/37/42/BRNS.

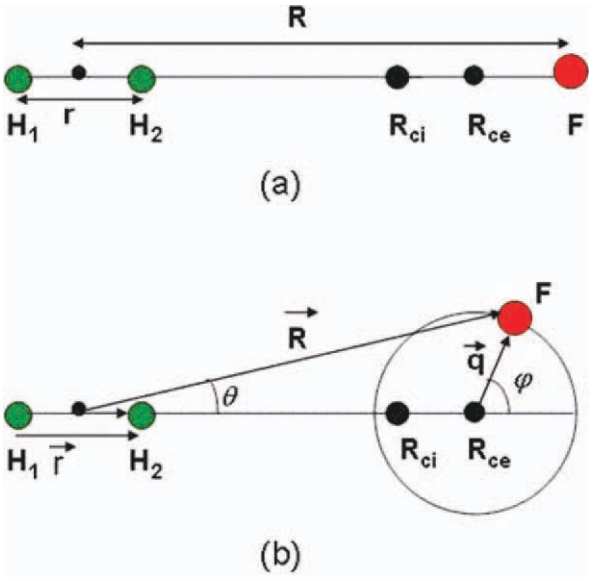

Figure 1. A schematic picture of the system of coordinates: a) positions of atoms, point of (1,2) CI and the center of all circular contours. b) System of coordinates: $(R,\theta|r)$ vs. $(\varphi,q|r)$. In this figure, atoms F, H_1, and H_2 stand for atoms A, B, and C, respectively, mentioned in the text. [Color figure can be viewed in the online issue, which is available at wileyonlinelibrary.com.]

the center-of-mass of the diatom, and θ is the angle between the two corresponding vectors **r** and **R** (see Fig. 1b). To study the nonadiabatic coupling terms (NACT), we break-up the three-dimensional configuration space and present it as a series of two-dimensional configuration spaces, which are chosen to be planes. Each plane is parameterized by a fixed value of *r*. This parameterization leaves, two of the three coordinates, *R* and θ, free to describe the position of the third atom, A, on that plane. Atom A serves as a test particle to examine the values of the NACTs, $\tau_{jk}(R,\theta|r)$ at a given series of grid points. Consequently, atom A is allowed to move freely on that plane, whereas atoms B and C are fixed so that $\mathbf{r} = \mathbf{R}_{BC}$. It is important to mention that to obtain the NACTs for the complete three-dimensional configuration space, the value of *r* is varied systematically along a given grid. However, the study of the NACTs, in each plane, is done independently.

The system we intend to study is made-up of three states: the lowest state is a Σ-state and the two upper states are Π-states. Next, we assume that the two lowest states, namely, the Σ-state and one of Π-states (designated as 1A′ and 2A′, respectively) form a JT CI which is located on the collinear axis and the two upper Π-states (designated as 2A′ and 2A″, respectively), which are known to become degenerate along the collinear tri-atom axis, form a line of RT CIs along this axis. According to the JT terminology,[19] such a line of degeneracy points is called a seam, and therefore, the RT study is usually performed using closed contours, Λ, that surrounds the collinear seam.[12–14] To be more specific, just like in the study of the JT effect,[19,20] we may calculate the corresponding RT-NACTs and follow their behavior along open and/or closed Λ-contours. However, this is not the study to be done in the present treatment. As the study of the JT-NACTs is performed in planes formed by the three atoms (which naturally contain also the collinear axis), there is no room to consider RT-NACTs along, the aforementioned, contours, Λ. Instead, we study the RT-NACTs, just like the JT-NACTs, only along Γ-contours located in these planes. As expected, these contours intersect the collinear axis (at two points) and at these intersection points we reveal the RT effect, as will be explained later. As the two types of NACTs, the JT-NACT and the RT-NACT, are associated with the collinear axis, it is expected that they are strongly entangled (see a general discussion on this issue in Ref. [21]).

The two-state system

The two-state ADT angle, $\gamma(\mathbf{s}|\Gamma)$ is calculated via line-integrals of the form[20]:

$$\gamma(\mathbf{s}|\Gamma) = \int_{\mathbf{s}_0}^{\mathbf{s}} \tau(\mathbf{s}'|\Gamma)\cdot d\mathbf{s}' \tag{1}$$

where $\tau(\mathbf{s})(=\tau_{ij}(\mathbf{s})) = \langle\zeta_i(\mathbf{s})|\nabla\zeta_j(\mathbf{s})\rangle$, $\zeta_i(\varphi|q)$ and $\zeta_j(\varphi|q)$ are the eigenfunctions related to the two interacting states ζ_i and ζ_j and ∇ is the Grad operator. Here, the integration is performed along a contour, Γ, located in the planar configuration space (the two points **s** and $\mathbf{s}_0$ are on Γ) and the dot stands for a scalar product. It is noticed that the tangential component is the only component relevant for calculation of the ADT angle. Equation (1) was applied for both, the JT-NACTs[2–11] and the RT-NACTs.[12–14]

To calculate the NACTs for this study, we choose a point on the collinear axis and assume the various contours, Γ, to be circles, which eventually cover the planar configuration space relevant for our study, all having the same center. The circles are defined in terms of the two polar coordinates (q,φ) which differ from (R,θ); see Fig. 1). As the ADT angle is determined only by the tangential component along Γ and because Γ is a circle, the equation for $\gamma(q,\varphi)$ simplifies to become[22]:

$$\gamma(\varphi|q) = \int_0^{\varphi} \tau_\varphi(\varphi\prime|q)d\varphi\prime \tag{2}$$

where $\tau_\varphi(\varphi|q)/q$ is the angular component of the corresponding NACT with the operator, τ_φ defined as $\tau_{\phi ij}(\phi|q) = \langle\zeta_i(\phi|q)|(\partial/\partial\phi)\zeta_j(\phi|q)\rangle$. The two systems of coordinates (q,φ) and (R,θ), for a given *r*-value, are connected *via* simple geometrical relations.

The RT effect and the three-state system

Whereas the calculations of two-state JT-NACTs in a plane is well-known and also straightforward, we, mainly, concentrate on the RT-NACT along the same planar circle, Γ. As the collinear axis is a straight line along the infinite interval $-\infty < R < +\infty$, each circle in that plane intersects this line at two points, that is, at $\varphi = 0$ and at $\varphi = \pi$ (see Fig. 1b). It is well-known that at each such intersection point, along a short interval

perpendicular to the collinear axis, is formed a non zero NACT (in this case, an angular NACT) with features reminiscent of a Dirac δ-function (this finding was established on various occasions—see Ref. [23]). Thus, our first tendency is to assume that the angular RT-NACTs in the planar configuration space take the form:

$$\tau_{\varphi}^{\mathrm{RT}}(\varphi|q,\Gamma)=\frac{\pi}{2}\delta(\varphi-\vartheta) \tag{3a}$$

for any circle Γ with a radius q (here ϑ designates the intersection points and is either zero or π—see Fig. 1b). Equation (3a) has to be applied with some care because as it stands it yields, for any circle, a quantized Berry phase ($=\pi$) to be expected for an undisturbed RT effect along Γ. However, in "The three-state model" section, we assumed the existence of a JT CI on the collinear axis, and therefore, the RT effect is most likely being disturbed by that CI (a detailed discussion on this phenomenon is given in Ref. [21]). Consequently, the quantization is disturbed, and to achieve that feature Eq. (3a) has to be modified. The most straightforward way to do that is to assume:

$$\tau_{\varphi}^{\mathrm{RT}}(\varphi|q,\Gamma)=\frac{\pi}{2}\eta\delta(\varphi-\pi) \tag{3b}$$

where η is a parameter expected to be smaller than 1. In what follows, Eq. (3b) is termed as the quasi-Dirac δ-function.

Following the presented three-state model in "The three-state model" section, we assert that the system contains the primary NACT, τ_{12} (formed by the two lower states 1A′ and 2A′) and two additional NACTs associated with the upper state 2A″, namely, τ_{23} and τ_{13}. These three NACTs are responsible for creating three Euler angles γ_{12}, γ_{23}, and γ_{13}. Appendix B shows that only two Euler angles are relevant for our study and they are determined by the following two coupled equations:

$$\nabla\gamma_{12}=-\tau_{12}-\tan\gamma_{23}(-\tau_{13}\cos\gamma_{12}+\tau_{23}\sin\gamma_{12}) \tag{4a}$$

$$\nabla\gamma_{23}=-(\tau_{23}\cos\gamma_{12}+\tau_{13}\sin\gamma_{12}) \tag{4b}$$

Equation (4) contain two significant physical messages: (1) the primary angle is γ_{12}; (2) it explicitly reveals the secondary effects of the two other NACTs on its formation.

According to the model presented earlier, τ_{12} is identified as the angular JT NACT, which couples the two (lower) JT states and, therefore, is designated as τ^{JT} and τ_{23} is identified as the angular RT-NACT, which couples the two corresponding RT-states and is designated as τ^{RT}. In this scheme, τ_{13}, which couples 1A′ and 2A″, is identically zero and therefore is ignored. Consequently, Eq. (4) become:

$$\frac{\partial\gamma_{12}(\varphi)}{\partial\varphi}=-\tau^{\mathrm{JT}}(\varphi)-\tau^{\mathrm{RT}}(\varphi)\sin\gamma_{12}(\varphi)\tan\gamma_{23}(\varphi) \tag{5a}$$

$$\frac{\partial\gamma_{23}(\varphi)}{\partial\varphi}=-\tau^{\mathrm{RT}}(\varphi)\cos\gamma_{12}(\varphi) \tag{5b}$$

Usually, the two above coupled equations have to be solved numerically. However, in this case, τ^{RT} is a Dirac δ-function [see Eq. (3a)] or a quasi-Dirac δ-function [see Eq. (3b)] and therefore can be solved analytically.

We start the solution process for the first case [Eq. (3a)]. Straightforward integration of Eq. (5a) yields the following solution for, $\gamma_{12}(\varphi|q,\Gamma)$:

$$\gamma_{12}(\varphi|q,\Gamma)=\gamma_{12}^{(0)}(\varphi|q,\Gamma)-\chi(\varphi|q,\Gamma) \tag{6}$$

where $\gamma_{12}^{(0)}(\varphi|q,\Gamma)$ is the usual two-state ADT angle given in the form [see also Eq. (2)]:

$$\gamma_{12}^{(0)}(\varphi|q,\Gamma)=-\int_0^{\varphi}\tau^{\mathrm{JT}}(\varphi\prime|q,\Gamma)d\varphi\prime \tag{7}$$

and$\chi(\varphi|q,\Gamma)$ is expressed by the product:

$$\chi(\varphi|q,\Gamma)=\Theta(\varphi-\pi)G(\varphi=\pi|q,\Gamma) \tag{8}$$

which follows from a straightforward integration of Eq. (5b). Here:

$$G(\varphi=\pi|q,\Gamma)=\tan\left\{-\frac{\pi}{2}\cos[\gamma_{12}^{(0)}(\varphi=\pi)]\right\}\sin\{\gamma_{12}^{(0)}(\varphi=\pi)\} \tag{9}$$

and $\Theta(\varphi-\pi)$ is a Heaviside (step) function defined as:

$$\Theta(\varphi-\pi)=\frac{\pi}{2}\begin{cases}0; & \varphi<\pi\\ 1; & \varphi>\pi\end{cases} \tag{10}$$

The solution for $\gamma_{12}(\varphi|q,\Gamma)$ is in fact identical to the one obtained by solving the two-state equation [cf. Eq. (6) and Eq. (7) with Eq. (2)] but which is shifted, vertically, at $\varphi=\pi$, by an amount:

$$\chi(\varphi=\pi)=\frac{\pi}{2}\tan\left\{-\frac{\pi}{2}\cos[\gamma_{12}^{(0)}(\varphi=\pi)]\right\}\sin\{\gamma_{12}^{(0)}(\varphi=\pi)\} \tag{11}$$

where the shift is solely caused by τ^{RT}. As $\left|\gamma_{12}^{(0)}(\varphi=\pi|q,\Gamma)\right|$ has to be larger than $\pi/2$ (to guarantee the quantization—see Appendix A), it is noticed that the two functions, $\chi(\varphi=\pi)$ and $\gamma_{12}^{(0)}(\varphi=\pi|q,\Gamma)$, have to maintain the same sign.

In what follows $\chi(\varphi=\pi)$ will be termed as the RT vertical shift (RTVS).

Short Summary. We found that the effect of the RT-NACT, as given in Eq. (3a), is shifting the unperturbed, two-state $\gamma_{12}^{(0)}(\varphi|q,\Gamma)$, at $\varphi=\pi$, vertically downward (or upward in case $\gamma_{12}^{(0)}$ is negative) by an amount $\chi(\varphi=\pi)$ given in Eq. (11). A similar shift is expected at $\varphi=0$, unless $\gamma_{12}^{(0)}(\varphi|q,\Gamma)$, at $\varphi=0$, is zero. Later, it will be shown that, indeed, $\gamma_{12}^{(0)}(\varphi=0|q,\Gamma)=0$.

Analysis of the RTVS

In order for the theory to be relevant, the RTVS has to be such that the resulting ADT angles fulfill two conditions:

a. The value of $\gamma_{12}(\varphi|q,\Gamma)$ in Eq. (6) with the RTVS given in Eq. (11) has to yield, at $\varphi=2\pi$, a quantized end-of-the-contour ADT angle, namely:

$$\gamma_{12}(\varphi=2\pi|q,\Gamma)=\alpha(q,\Gamma)=n\pi \tag{12}$$

where n is an integer (or zero).

b. The RTVS has to be such that the diabatic potentials, at $\varphi = \pi$ (where $\gamma_{12}(\varphi|q,\Gamma)$ suffers a vertical, discontinuous jump), are single-valued. Thus, if $\gamma_{12}^{(0,0)}(\varphi|q,\Gamma)$ is the value of $\gamma_{12}(\varphi|q,\Gamma)$ following the vertical jump, namely:

$$\gamma_{12}^{(0,0)}(\varphi = \pi) = \gamma_{12}^{(0)}(\varphi = \pi) - \chi(\varphi = \pi) \tag{13}$$

the sufficient conditions for the single-valuedness of the diabatic potentials is:

$$\sin\gamma_{12}^{(0,0)}(\varphi = \pi) = \sin\gamma_{12}^{(0)}(\varphi = \pi) \tag{14}$$

and a similar condition for the cosine function.

In Appendix A, it is shown that the two conditions, (a) and (b), are satisfied if and only if the RTVS takes the form:

$$\chi(\varphi = \pi|q,\Gamma) = 2\left\{\gamma_{12}^{(0)}(\varphi = \pi|q,\Gamma) \pm \pi/2\right\} \tag{15}$$

where the plus sign applies for the case that $\gamma_{12}^{(0)}(\varphi = \pi|q,\Gamma)$ is negative and the minus sign when this angle is positive.

The difficulty to worry about is that $\chi(\varphi = \pi|q,\Gamma)$ as derived in the previous section and presented in Eq. (11) is not guaranteed to satisfy Eq. (15). Therefore, in the rest of this section we examine under what conditions, the two formulae [in Eqs. (11) and (15)] are compatible. The analysis will be done for the case that $\gamma_{12}^{(0)}(\varphi = \pi|q,\Gamma)$ is positive.

To keep this study analytic, we assume that $\gamma_{12}^{(0)}(\varphi = \pi)$ deviates only slightly from $\pi/2$, namely:

$$\gamma_{12}^{(0)}(\varphi = \pi) = (\pi/2) + \varepsilon \tag{16}$$

where ε is a negligible small, but otherwise, an arbitrary magnitude. Substituting Eq. (16) in Eq. (15), yields for RTVS the value 2ε but substituting it in Eq. (11) and keeping only linear terms in ε yields, for RTVS, the value:

$$\chi(\phi = \pi) = (\pi/2)^2\varepsilon = 2.56\varepsilon \tag{17}$$

In other words, the theoretical value that follows from Eq. (11) is too large (2.56ε vs. 2ε). The value of $\chi(\varphi = \pi)$, in Eq. (17), is associated with the fact that the RT-NACT is a pure Dirac δ-function [see Eq. (3a)] an assumption that causes the RTVS to be too large.

Consequently, we try to solve Eq. (5) for the quasi-Dirac δ-function given in Eq. (3b). Doing that we obtain, for $\chi(\varphi = \pi)$, the following extended result:

$$\chi^{(\eta)}(\varphi = \pi) = \frac{\pi}{2}\eta\tan\left\{-\frac{\pi}{2}\eta\cos[\gamma_{12}^{(0)}(\varphi = \pi)]\right\}\sin\{\gamma_{12}^{(0)}(\varphi = \pi)\} \tag{18}$$

Repeating the treatment of the above perturbed case [see Eq. (16)], we get for the modified value of RTVS the result:

$$\chi^{(\eta)}(\varphi = \pi) = \left(\frac{\pi}{2}\eta\right)^2\varepsilon \tag{19}$$

Demanding that the coefficient of ε is 2, implies that

$$\left(\frac{\pi}{2}\eta\right)^2 = 2 \quad \rightarrow \quad \eta = \frac{2\sqrt{2}}{\pi} \sim 0.9003 \tag{20}$$

Short Summary. In this section, we derived a theoretical expression for the modified, two-state, ADT angle [see Eqs. (6), (7), and (11)]. In order for this expression to be consistent with the requirement of having single-valued diabatic potentials, the RT-NACT [in Eq. (3a)] has to be changed. Applying the modified value [in Eq. (3b)] produces, for a suitable value of η [Eq. (20)], the two-state ADT angle which is compatible with these requirements (at least for small deviations). The parameter η can be interpreted as the normalization factor for the RT-NACT.

Numerical Results

In the numerical part of our study, we concentrate on η with the aim of revealing to what extent its values remain stable while varying characteristic parameters related to the JT-NACT. For this sake, we consider the $H_2 + F$ system (the model described in "The three-state model" section was constructed to be suitable for this system) for which the JT-NACTs are generated by MOLPRO (A package of *ab initio* programs written by H.-J. Werner, P. J. Knowles with contributions from J. Almlöf, et al.; see Appendix A for details). In this system, the JT CI and the corresponding NACT are formed by a Σ-state, assigned as $1A'$, and one of the two Π-states (with the same symmetry) assigned as $2A'$. The RT CIs are formed by the corresponding two degenerate Π-states, designated as $2A'$ and $2A''$ and, as usual, are located along the (collinear) HHF axis. The corresponding RT-NACTs that are required for this study are not calculated but derived theoretically as described in "The two-state system" and "The RT effect and the three-state system" sections. Saying all that still some explanation has to be given about this numerical issue. As it turned out, MOLPRO was not always detailed enough in supplying the entire smooth curve for this coupling. This is in contradiction to what we encountered during a similar study as reported in Ref. [9(a)].

At this stage, we refer to the fact that PESs for the $F + H_2$ system were calculated by numerous groups during the last half-century. We mention here mainly the study by Stark and Werner (SW) who produced the most relevant up-to-date ground state potential for this system. SW also extended their calculations in two ways[24]: (a) they revealed the existence of a JT CI located on the collinear axis in vicinity of $R \sim 5.5$ au (mentioned earlier while constructing the model); (b) they derived the first set of (the two lowest) diabatic potentials and the corresponding diabatic coupling term for this system.

Unfortunately, their diabatic potentials may not be meaningful and hardly rigorous as the required NACTs for this purpose were derived by analyzing the coefficients in the configuration interaction expansion of the FH_2 wave function[24–26] (somewhat reminiscent of an approach based on the transition dipole moments[27]) instead of using the Born–Oppenheimer (BO) NACTs.[28]

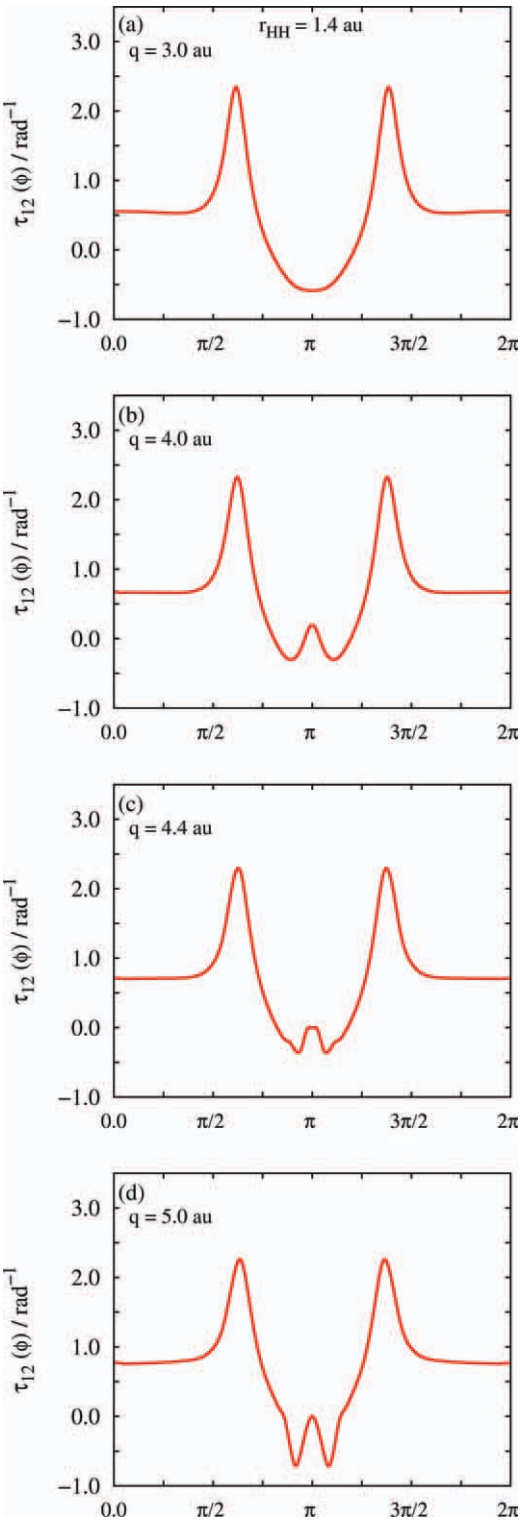

Figure 2. Angular NACTs, $\tau_{\varphi 12}$ $(\varphi|q)$, for circular contours located at $R = R_{ce} = 6$ au. Along the interval $0 \leq \varphi \leq 2\pi$: a) results for $q = 3$ au; b) results for $q = 4$ au; c) results for $q = 4.4$ au; (d) results for $q = 5$ au. The calculations are done for the planar configuration space at $r = 1.4$ au (see Fig. 1). Note that the main part of the NACTs is positive and only in the vicinity of $\varphi \sim \pi$ the NACTs become negative. [Color figure can be viewed in the online issue, which is available at wileyonlinelibrary.com.]

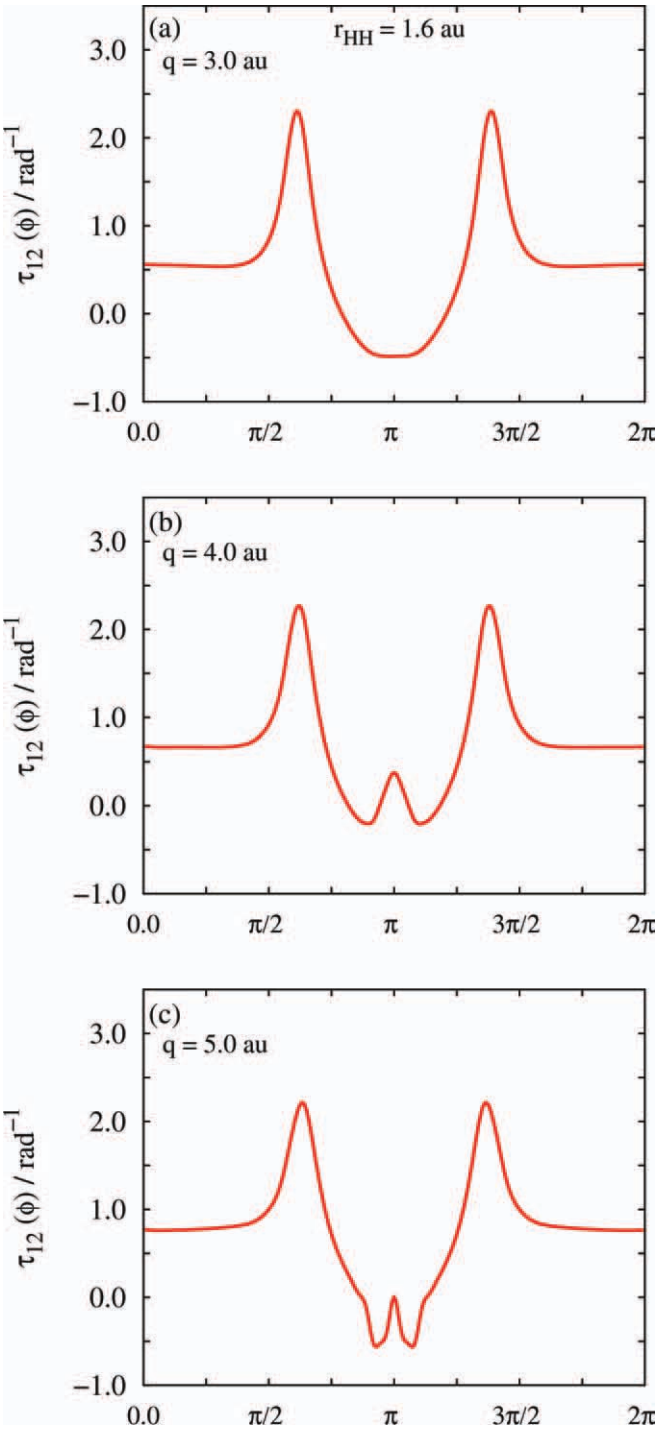

Figure 3. Angular NACTs, $\tau_{\varphi 12}$ $(\varphi|q)$, for circular contours located at $R = R_{ce} = 6$ au. Along the interval $0 \leq \varphi \leq 2\pi$: a) results for $q = 3$ au; b) results for $q = 4$ au; c) results for $q = 5$ au. The calculations are done for the planar configuration space at $r = 1.6$ au (see Fig. 1). Note that the main part of the NACTs is positive and only in the vicinity of $\varphi \sim \pi$ the NACTs become negative. [Color figure can be viewed in the online issue, which is available at wileyonlinelibrary.com.]

In contrast to the just mentioned ADT treatment by Werner et al. for the F + H_2 system, most of the treatments of other molecular systems are done by applying the original BO-NACTs.[1–14,18–23,29–47] This study for the F + H_2 system is the first that uses BO-NACTs for the diabatization of this system.

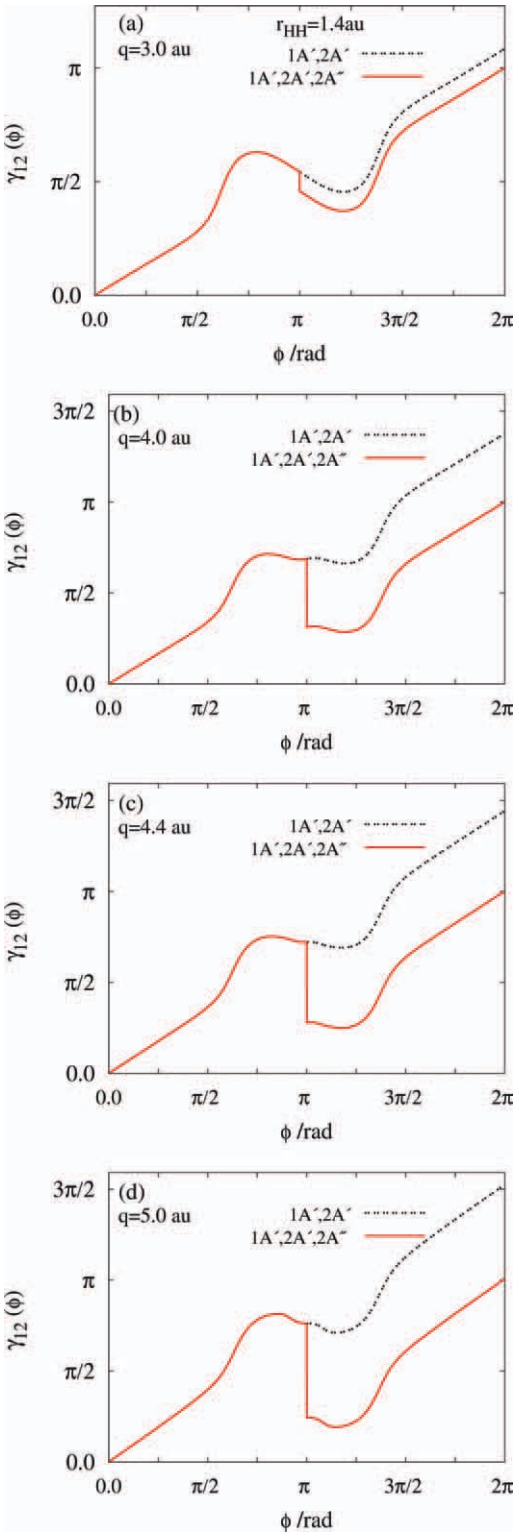

Figure 4. Adiabatic-to-diabatic-transformation (mixing) angle, γ_{12} ($\varphi|q$), for circular contours at $R = R_{ce} = 6$ au along the interval $0 \leq \varphi \leq 2\pi$. a) Results for $q = 3$ au; b) results for $q = 4$ au; c) results for $q = 4.4$ au; d) results for $q = 5$ au. The calculations are done for the planar configuration space at $r = 1.4$ au (see Fig. 1): - - - - two-state results, $\gamma_{12}^{(0)}$ ($\varphi|q$) as calculated using Eq. (7). ----- Modified two-state results γ_{12} ($\varphi|q$) as calculated using Eq. (21). [Color figure can be viewed in the online issue, which is available at wileyonlinelibrary.com.]

The results to be reported in this article are obtained for two different planar configuration spaces: one determined by r ($= R_{HH}$) $= 1.4$ au and the other by $r = 1.6$ au. For these two configurations, the system is dominated, to the best of our knowledge, by one (1,2) JT CI located on the collinear axis at the vicinity of $R = R_{CI} \sim 5.5$ au (see Fig. 1) and the RT-NACTs along the collinear axis.

As discussed earlier, the theoretical study and the calculations are done along closed circular contours. All circles have their centers at the same fixed point, $R = R_c = 6$ au on the collinear axis. This common center is chosen in such a way as to guarantee that these circles cover the whole planar configuration space of interest.

The (1,2) JT-NACTs along closed circles

Figures 2 and 3 present angular JT-NACTs as calculated along seven different (closed) circles: Figure 2 presents results for one planar case where $r_{HH} = 1.4$ au (for four circles with the radii: $q = 3.0$, 4.0, 4.4, and 5.0 au) and Figure 3 presents results for a second planar case where $r_{HH} = 1.6$ au (for three circles with the radii: $q = 3.0$, 4.0, and 5.0 au).

The most characteristic feature to be noticed is the symmetric structure of the NACTs, which indicates that the just mentioned JT CI is located on the collinear axis. Each curve shows two peaks—one for NACTs mainly concentrated in the (π/2,π) angular sector and the other in the (π,3π/2) sector. The structure as a whole is tilted toward the HHF axis. These two facts support one of our earlier assumption namely, that for any circle, in the vicinity of $\varphi = 0$, the JT-NACT is ~ 0 [which implies that no RTVS takes place at $\varphi = 0$—see Eq. (11) or Eq. (18)]. In addition, we notice that all NACTs calculated for different contours become negative along a short arc around $\varphi = \pi$. In numerous, previous, studies we could, unambiguously, attribute this feature to the fact that other NACTs formed by higher states are (topologically) close enough to affect the NACTs under consideration—in our case the (1,2) JT-NACT. Situations like that were observed in Ref. [3(a), see Fig. 1(g)], in Ref. [4(a), see Fig. 7(e)], and in Ref. [5(a), see Fig. 1(b)]. Thus, like in these cases, also, here the two-state JT-NACTs are affected by NACTs formed by higher states—in this case, to our surprise, by RT-NACTs.

The (1,2) ADT angles along closed circles

The (1,2) ADT angles are presented in Figures 4 and 5: Figure 4 gives results for the case that $r_{HH} = 1.4$ au (for four circles with the radii: $q = 3.0$, 4.0, 4.4, and 5.0 au) and Figure 5 gives results for the case $r_{HH} = 1.6$ au (for three circles with the radii: $q = 3.0$, 4.0, and 5.0 au). In each panel, two curves are shown. One of them is calculated applying the two-state formula in Eq. (7) [see also Eq. (2)] along the full circular range (0,2π). It is noticed that all two-state curves are essentially uniformly increasing functions of φ, and the rate of increase is steeper the larger is the value of q.

One of the features that we expect to see due to the calculations is that the end-of-the-closed-contour ADT angle

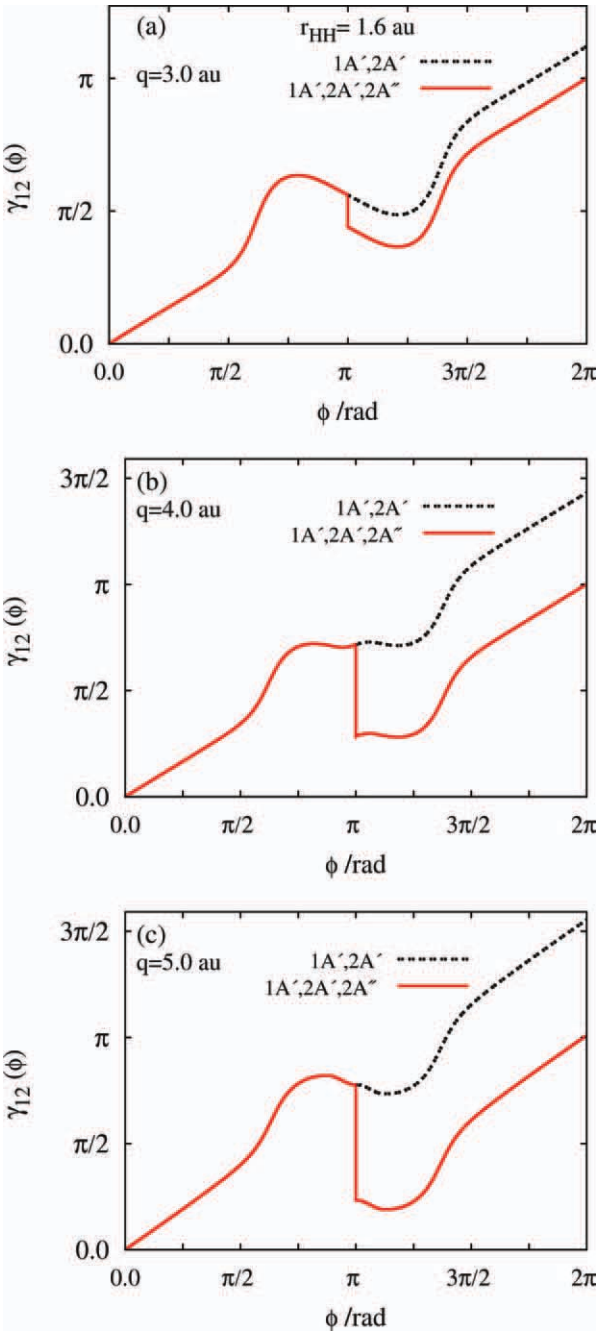

Figure 5. Adiabatic-to-diabatic-transformation (mixing) angle, γ_{12} ($\varphi|q$), for circular contours at $R = R_{ce} = 6$ au along the interval $0 \leq \varphi \leq 2\pi$. a) Results for $q = 3$ au; b) results for $q = 4$ au; c) results for $q = 5$ au. The calculations are done for the planar configuration space at $r = 1.6$ au (see Fig. 1): - - - - Two-state results, $\gamma_{12}^{(0)}$ ($\varphi|q$) as calculated using Eq. (7). ----- Modified two-state results γ_{12} ($\varphi|q$) as calculated using Eq. (21). [Color figure can be viewed in the online issue, which is available at wileyonlinelibrary.com.]

[identified with the Berry phase[17] and designated as $\alpha(q,\Gamma)$] becomes an integer multiple of π (see Appendix A). As is noticed, only in case of $q = 3$ au, we get a value close to π, namely, $\alpha(q = 3$ au, $\Gamma) \sim \pi$, whereas in all other cases (for which $q > 3$ au) the values of α are larger than π. It is important to emphasize that in those cases where $q < 3$ au the calculations produced, consistently, the quantized result: $\alpha(q,\Gamma) = \pi$.

As discussed in "The two-state system" and "The RT effect and the three-state system" sections, the way to remedy the situation, for the ill-conditioned cases, is to include the RT NACT formed by the next closest states and calculate the corresponding ADT angle by solving Eq. (5) [instead of Eq. (2)]. As the RT-NACTs are located along the collinear axis they form, at each point that the contour Γ intersects this axis, a singular NACT [see Eq. (3b)] for which Eq. (5) are solved. The solution indicates that the RT-NACT, due to its singular nature, affects the JT NACT only at the intersection point $\varphi = \pi$. This effect resembles itself as a vertical (downward) shift, the RTVS, $\chi(\varphi = \pi)$, of the ADT curves so that the modified two-state ADT function takes the form:

$$\gamma_{12}(\varphi|q,\Gamma) = \begin{cases} \gamma_{12}^{(0)}(\varphi|q,\Gamma)\,; 0 \leq \varphi \leq \pi \\ \gamma_{12}^{(0)}(\varphi|q,\Gamma) - \chi^{(\eta)}(\varphi = \pi|q,\Gamma)\,; \pi \leq \varphi \leq 2\pi \end{cases} \tag{21}$$

where $\gamma_{12}^{(0)}$ and $\chi^{(\eta)}$ are given by Eqs. (7) and (18), respectively. To estimate the size of the vertical shift $\chi^{(\eta)}(\varphi = \pi)$, we analyzed, in "The RT effect and the three-state system" section, the extreme case of an infinitely small differential shift and revealed that the RT-NACT defined in Eq. (3b) satisfies the ultimate requirement for single-valued diabatic potentials when the new parameter, η, becomes $\eta = 2\sqrt{2}/\pi$ [see Eq. (20)].

The numerical study is devoted to establish the validity of this value for common situations (where the deviations are of any size). It is straightforward to find for each $\gamma_{12}^{(0)}(\varphi = \pi)$ the corresponding RTVS that guarantees the quantized Berry phase by using the relation presented in Eq. (15). Indeed for these values (listed in the third column in Table 1), we draw the various curves, in Figures 4 and 5, using Eq. (21). Thus, knowing the RTVS for any case, we may apply Eq. (18) to extract the corresponding value of η. In this article, we decided to apply a different approach. In Table 1 are compared, for each case, two values of RTVS: (1) as mentioned before by applying Eq. (15) [for which we need only $\gamma_{12}^{(0)}(\varphi = \pi)$]; (2) calculating the value of $\chi^{(\eta)}(\varphi = \pi)$ using Eq. (18) for the same value of $\gamma_{12}^{(0)}(\varphi = \pi)$and assuming $\eta = 2\sqrt{2}/\pi$. The comparison between the two kinds of RTVSs is presented in the last two columns of Table 1. It is well noticed that the two types of results are very close and only in the last case we observe a small deviation of less than 2%. This small

Table 1. The Renner–Teller vertical shift.

r_{HH} (au)	q (au)	$\gamma_{12}^{(0)}$ (Rad)	$\chi(\varphi = \pi)$ (Numerical)[a]	$\chi^{(\eta)}(\varphi = \pi)$ (Theory)[a]
1.4	3.0	1.70	0.26	0.26
	4.0	2.16	1.18	1.18
	4.4	2.27	1.40	1.41
	5.0	2.40	1.66	1.63
1.6	3.0	1.76	0.38	0.38
	4.0	2.25	1.36	1.35
	5.0	2.44	1.74	1.71

a [a] Results in Rads.

deviation (like, eventually the other minor ones) can be attributed to the effect of other NACTs expected in the planar configuration spaces, or also to inaccuracies due to MOLPRO. In what follows, η is termed as Jahn–Renner Coupling Parameter (JRCP).

Summary and Conclusions

For more than a decade, we study the effect of higher states on the lower two-state NACTs. Essentially, all studies were performed using ADT matrices (see Appendix B) an approach which, from numerical point of view, is straightforward.[19,20] However, from theoretical point of view, the application of the ADT matrices do not satisfy our curiosity concerning the interplay between the lower NACT and those above it. First attempts in this direction were made a few years ago when we started calculating Euler angles (see Appendix B), which form these ADT (orthogonal) matrices.[18]

A better understanding of this situation was achieved in our more recent study performed for the H_2CN molecule[14] for which we treated the RT/JT-NACTs of this system. There, we showed that the relevance of two-state ADT angles, as calculated by the line-integral given in Eq. (2), converges much better to its quantized value by adding NACTs formed by higher states and solving equations similar to Eq. (4) for two Euler angles or more. The extent of this improvements is presented recently in Ref. [14] and also see Figures 6 and 7 in Ref. [18].

The approach used in Ref. [14] is used here. This study is not only the first of its kind in which is reported the interplay between JT-NACTs and RT-NACTs and their role in determining the relevant (1,2) ADT angles but is also the first of its kind in which is reported the effect of a singular NACT on two-state JT ADT angles. The fact that the upper NACT appears as a quasi-Dirac δ-function enabled a semi-analytical solution for the improved two-state ADT angles.

The present treatment, performed for the $F + H_2$ system, revealed the existence of a novel parameter, η, the JRCP, which yields, in an unambiguous way, the right intensity of the coupling for the quasi-Dirac δ-function [Eq. (3b)] responsible for the fact that the corresponding Berry phase converges uniformly to π. This study implies that the numerical value of this parameter, is $\eta = 2\sqrt{2}/\pi$ (= 0.9003) and that there is a good possibility that this value is characteristic for all tri-atomic systems with a similar structure and therefore, eventually, can be considered as a novel molecular constant.

Appendix A

On the Single-Valuedness of the Diabatic Potentials

Given the two adiabatic PESs $u_j(\varphi|q)$; $j = 1,2$, the corresponding two-state diabatic potentials $V_1(\varphi|q)$, $V_2(\varphi|q)$, and $V_{12}(\varphi|q)$, are derived from the following set of equations[48]:

$$\begin{aligned} V_1(\gamma(\varphi|q)) &= u_1(\varphi|q)\cos^2\gamma(\varphi|q)+u_2(\varphi|q)\sin^2\gamma(\varphi|q) \\ V_2(\gamma(\varphi|q)) &= u_1(\varphi|q)\sin^2\gamma(\varphi|q)+u_2(\varphi|q)\cos^2\gamma(\varphi|q) \\ V_{12}(\gamma(\varphi|q)) &= (1/2)(u_2(\varphi|q)-u_1(\varphi|q))\sin(2\gamma(\varphi|q)) \end{aligned} \quad \text{(A1)}$$

where γ is given in Eq. (1). The transformation that yields the diabatic potentials is presented explicitly to show that to guarantee the single-valuedness of these potentials along closed circles the angle $\gamma(\varphi|q)$ has to be quantized,[15,16] in other words, the value of $\gamma(\varphi|q)$ at $\varphi = 2\pi$ has to be equal to $n\pi$ where n is an integer (or zero). In realistic cases, this requirement may not always be satisfied due to the effect of NACTs formed by higher states. To overcome this difficulty, higher states and their NACTs have to be incorporated in the diabatization process so that usually we end-up with an N-state diabatization, where $N > 2$. This, in turn, requires performing the nuclear scattering treatment with N (diabatic) states.

In this study, we take advantage of an approach in which are solved two Euler-type angles to study the effect (perturbation) of a third state on a system of two coupled states.[14] Thus, although the two-state diabatization [which yield $V_1(\varphi|q)$, $V_2(\varphi|q)$, and $V_{12}(\varphi|q)$] is based on three interacting states, the nuclear dynamic treatment, can be performed for two (diabatic)-states (as long as the quantization is satisfied). The only difference is that now $\gamma(\varphi|q)$ is a solution of two coupled equations [and not the one given in Eq. (1) or Eq. (2)]. For more details, see Refs. [14,18].

Equation (5) are the ones to be solved for the present case and it is well noticed from the analysis given in "The two-state system" section that the effect of the second (RT) NACT is shifting the original (undisturbed) two-state $\gamma_{12}^{(0)}(\varphi|q,\Gamma)$ vertically downward (or upward in case it is negative) at $\varphi = \pi$. This vertical shift [see Eq. (11)], recognized by the acronym RTVS has to be such that the modified two-state ADT angle, at $\varphi = 2\pi$, becomes π (or $n\pi$ where n is an integer).

In "The RT effect and the three-state system" section is analyzed the, so-called, perturbed case for which $\gamma_{12}^{(0)}(\varphi = \pi|q,\Gamma)$ deviates only slightly from $(\pi/2)$ so that the deviation, ε [see Eq. (16)], is negligible small. The analysis shows, unambiguously, that for the RT-NACT defined in Eq. (3a), the resulting RTVS is too large thus causing $\gamma_{12}^{(0)}(\varphi = 2\pi|q,\Gamma)$ to be consistently smaller than π. This fact implies that the RT-NACT in Eq. (3a) is too strong. One way to overcome this difficulty is to replace Eq. (3a) by the following expression:

$$\tau_\phi^{\mathrm{RT}}(\varphi|q,\Gamma) = \frac{\pi}{2}\eta\delta(\varphi-\pi) \quad \text{(A2)}$$

where η is smaller than 1. Using Eq. (A2) and solving again Eq. (5) yields for $\chi^{(\eta)}(\varphi = \pi)$—the modified RTVS—a more general expression [see Eq. (18)]. The parameter η is, so far, unknown but demanding that for any, ε, the corresponding Berry phase, $\gamma_{12}^{(0)}(\varphi = 2\pi|q,\Gamma)$ is quantized (namely, equal to π) yields for η a fixed numerical value:

$$\eta = \frac{2\sqrt{2}}{\pi} \sim 0.9003 \quad \text{(A3)}$$

The analysis in "The RT effect and the three-state system" section, for the perturbed case, can be generalized by demanding that for any case the corresponding RTVS, $\chi^{(\eta)}(\varphi = \pi)$, has to guarantee a quantized $\gamma_{12}^{(0)}(\varphi = 2\pi|q,\Gamma)$. The

conditions for that to happen can be complicated but for a symmetric case it can be shown to happen if and only if:

$$\chi(\varphi=\pi|q,\Gamma)=2\left\{\gamma_{12}^{(0)}(\varphi=\pi|q,\Gamma)\pm\pi/2\right\} \tag{A4}$$

(the minus sign is for positive $\gamma_{12}^{(0)}(\varphi=\pi|q,\Gamma)$ and the plus sign for the negative case).

Another feature to worry about is that the diabatic PESs at $\varphi=\pi$ [where $\gamma_{12}(\varphi|q,\Gamma)$ suffers the discontinuous RTVS], are single-valued. Defining

$$\gamma_{12}^{(0,0)}(\varphi=\pi)=\gamma_{12}^{(0)}(\varphi=\pi)-\chi(\varphi=\pi) \tag{A5}$$

the sufficient conditions for that to happen are:

$$\sin\gamma_{12}^{(0,0)}(\varphi=\pi)=\sin\gamma_{12}^{(0)}(\varphi=\pi) \tag{A6a}$$

$$\cos\gamma_{12}^{(0,0)}(\varphi=\pi)=-\cos\gamma_{12}^{(0)}(\varphi=\pi) \tag{A6b}$$

Indeed, substituting Eqs. (A4) and (A5) in Eq. (A6) shows that the sufficient conditions are fulfilled. Next substituting Eq. (A6) in Eq. (A1) it is noticed that:

$$V_j(\gamma^{(0,0)}(\varphi|q))=V_j(\gamma^{(0)}(\varphi|q))j=1,2 \tag{A7a}$$

$$V_{12}(\gamma^{(0,0)}(\varphi|q))=-V_{1,2}(\gamma^{(0)}(\varphi|q)) \tag{A7b}$$

These relations guarantee the continuity of the diabatic potentials at the point of the RTVS.

Comment

During the theoretical analysis, we assumed that $|\gamma_{12}^{(0)}(\varphi=\pi|q,\Gamma)|>\pi/2$. In principle, this magnitude can, also, be smaller than $\pi/2$ but this would cause the sign of $\chi(\varphi=\pi)$ to differ from the sign of $\gamma_{12}^{(0)}(\varphi=\pi|q,\Gamma)$.

Appendix B

The ADT Matrix and the Euler Angles

Having the BO adiabatic (diagonal) potential matrix, $\mathbf{u}(\mathbf{s})$, the corresponding diabatic potential matrix $\mathbf{W}(\mathbf{s})$ is obtained following the ADT matrix, $\mathbf{A}(\mathbf{s})$[20(a)]:

$$\mathbf{W}(\mathbf{s})=\mathbf{A}^{\dagger}(\mathbf{s})\mathbf{u}(\mathbf{s})\mathbf{A}(\mathbf{s}) \tag{B1}$$

The ADT matrix is an orthogonal (unitary) matrix that fulfills the following first order differential (vector) equation[20(a)]

$$\nabla\mathbf{A}(\mathbf{s})+\tau(\mathbf{s})\mathbf{A}(\mathbf{s})=\mathbf{0} \tag{B2}$$

where $\tau(\mathbf{s})$ is the nonadiabatic coupling matrix with the elements as defined in Eq. (1). The solution of this equation can be written as an exponentiated line integral[20(b)]

$$\mathbf{A}(\mathbf{s}|\mathbf{s}_0,\Gamma)=\wp\exp\left(-\int_{\mathbf{s}_0}^{\mathbf{s}}d\mathbf{s}\cdot\tau(\mathbf{s}|\Gamma)\right)\mathbf{A}(\mathbf{s}_0) \tag{B3}$$

where $\wp$ is the ordering operator, $\mathbf{s}_0$ is the initial point of integration, Γ is the contour along which the solution of Eq. (B3) is required, the dot stands for a scalar product, and $\mathbf{A}(\mathbf{s}_0)$ is the initial value of $\mathbf{A}(\mathbf{s})$ on Γ. In what follows, $\mathbf{A}(\mathbf{s}_0)$ is assumed to be the unit matrix.

In case of circular contours, Eq. (B3) simplify to become:

$$\mathbf{A}(\varphi|q,\Gamma)=\wp\exp\left(-\int_0^{\varphi}d\varphi\tau_{\varphi}(\varphi|q,\Gamma)\right) \tag{B4}$$

where τ_{φ} is a matrix that contains elements defined in Eq. (2); see main text.

Next, we concentrate on the case of three interacting states which is treated in terms of a 3×3 **A**-matrix. As the **A**-matrices are orthogonal, the nine elements of the present matrix can be presented in terms of three angles, γ_{12}, γ_{13}, and γ_{23}, reminiscent of three Euler angles.[14,18,20(c)] To get the relevant form for the ADT matrix, **A** is presented as a product of three rotation matrices $\mathbf{Q}_{ij}(\gamma_{ij})$ ($i<j=2,3$) where the product $\mathbf{A}=\mathbf{Q}_{kl}\,\mathbf{Q}_{mn}\,\mathbf{Q}_{pq}$ can be written in any order. Substituting this product in Eq. (B2) yields three coupled first-order differential equations for the three corresponding quasi-Euler angles, γ_{ij}. The final set of equations as well as their solution depends on the order of the **Q**-matrices (there exist six different products).

In the analysis performed some time ago,[14,18] we attributed physical meaning mainly to those ADT angles γ_{12}, that are formed by sets of equations with the NACT, τ_{12}, being a free, isolated term. The reason is that these solutions produce an angle γ_{12} which is directly associated with the physical processes that happen on the lowest adiabatic PES, $u_1(\mathbf{s})$. Two such products: $\mathbf{A}=\mathbf{Q}_{12}\,\mathbf{Q}_{13}\,\mathbf{Q}_{23}$ and $\mathbf{A}=\mathbf{Q}_{12}\,\mathbf{Q}_{23}\,\mathbf{Q}_{13}$ yield sets of equations with a free τ_{12} and we chose the (second) product which leads to the following set of coupled equations (more on this issue can be found in Ref. [18]):

$$\begin{aligned}\nabla\gamma_{12}&=-\tau_{12}-\tan\gamma_{23}(-\tau_{13}\cos\gamma_{12}+\tau_{23}\sin\gamma_{12})\\ \nabla\gamma_{23}&=-(\tau_{23}\cos\gamma_{12}+\tau_{13}\sin\gamma_{12})\\ \nabla\gamma_{13}&=(\cos\gamma_{23})^{-1}(-\tau_{13}\cos\gamma_{12}+\tau_{23}\sin\gamma_{12})\end{aligned} \tag{B5}$$

It is well noticed that the first two equations form a closed set of equations that can be solved independently for γ_{12} and γ_{23}, whereas the last equation yields the solution for γ_{13}. As our main interest is in γ_{12}, we concentrate on the following two coupled equations:

$$\begin{aligned}\nabla\gamma_{12}&=-\tau_{12}-\tan\gamma_{23}(-\tau_{13}\cos\gamma_{12}+\tau_{23}\sin\gamma_{12})\\ \nabla\gamma_{23}&=-(\tau_{23}\cos\gamma_{12}+\tau_{13}\sin\gamma_{12})\end{aligned} \tag{B6}$$

Appendix C

The Numerical Treatment

Adiabatic PESs of the two lowest adiabatic states, $1^2A'$ and $2^2A'$ as well as the NACTs (along chosen circles) have been generated at multi reference configuration interaction (MRCI) level with Davidson correction[49] using MOLPRO program (A package of *ab initio* programs written by H.-J. Werner, P. J. Knowles with contributions from J. Almlöf, et al.). The active space has been chosen as

comprising of the 3σ–6σ orbitals, 1π valence orbitals and one additional set of correlating 2π orbitals. Care has been taken[24] to avoid the swap of 2σ and 3σ orbitals during the optimization of the orbitals at the complete active space self consistent field (CASSCF) level. The basis set used are: for the fluorine, we applied s and p functions from the cc-pV5Z set and d, f, and g functions from cc-pVQZ set augmented with diffuse s, p, d, f, and g functions. For the hydrogens, we used s functions from the cc-pV5Z set, and p and d functions from the cc-pVQZ set augmented with diffuse s and p functions. In this calculation, we used the active space including all seven valence electrons distributed on eight (8) orbitals.

Acknowledgments

A.D. acknowledges CSIR, India for research fellowship.

Keywords: nonadiabatic coupling terms · Jahn–Teller intersection · Renner–Teller intersection · potential energy surfaces · adiabatic to diabatic angle

How to cite this article: A. Das, D. Mukhopadhyay, S. Adhikari, M. Baer, *Int. J. Quantum Chem.* **2012,** *112,* 2561–2570. DOI: 10.1002/qua.23272

[1] C. A. Mead, *J. Chem. Phys.* **1983**, *78,* 807.
[2] (a) D. R. J. Yarkony, *Chem. Phys.* **1996**, *105,* 19456; (b) S. Mahapatra, H. J. Koppel, *Chem. Phys.* **1998**, *109,* 1721; (c) R. Abrol, A. Shaw, A. Kuppermann, D. R. Yarkony, *J. Chem. Phys.* **2001**, *115,* 4640; (d) S. Han, D. R. Yarkony, *J. Chem. Phys.* **2003**, *119,* 5058.
[3] (a) G. J. Halász, Á. Vibók, A. M. Mebel, M. Baer, *Chem. Phys. Lett.* **2002**, *358,* 163; (b) G. J. Halász, Á. Vibók, A. M. Mebel, M. Baer, *J. Chem. Phys.* **2003**, *118,* 3052; (c) M. Baer, T. Vertesi, G. J. Halász, Á. Vibók, S. Suhai, *Discuss Faraday Soc.* **2004**, *127,* 337; (d) T. Ve'rtesi, Á. Vibók, G. J. Halász, M. Baer, *J. Phys. B. At. Mol. Opt. Phys.* **2004**, *37,* 4603; (e) Z.-R. Xu, M. Baer, A. J. C. Varandas, *J. Chem. Phys.* **2000**, *112,* 2746.
[4] (a) A. M. Mebel, A. Yahalom, R. Englman, M. Baer, *J. Chem. Phys.* **2001**, *115,* 3673; (b) G. D. Billing, M. Baer, A. M. Mebel, *Chem. Phys. Lett.* **2003**, *372,* 1; (c) T. Ve'rtesi, E. Bene, *Chem. Phys. Lett.* **2004**, *392,* 17.
[5] (a) Á. Vibók, G. J. Halász, S. Suhai, M. Baer, *J. Chem. Phys.* **2005**, *122,* 134109; (b) J. Murrel, S. Carter, I. M. Mills, M. F. Guest, *Mol. Phys.* **1980**, *42,* 605; (c) G. Durand, X. Chapuisat, *Chem. Phys.* **1985**, *96,* 381; (d) A. J. Dobbyn, P. J. Knowles, *Mol. Phys.* **1997**, *91,* 1107; (e) D. R. Yarkony, *Mol. Phys.* **1998**, *93,* 971.
[6] (a) Á. Vibók, G. J. Halász, S. Suhai, D. K. Hoffman, D. J. Kouri, M. Baer, *J. Chem. Phys.* **2000**, *112,* 2746; (b) Á. Vibók, G. J. Halász, S. Suhai, D. K. Hoffman, D. J. Kouri, M. Baer, *J. Chem. Phys.* **2006**, *124,* 024312.
[7] (a) H. Koppel, *Faraday Discuss* **2004**, *127,* 35; (b) G. J. Halász, Á. Vibók, M. Baer, *Chem. Phys. Lett.* **2005**, *413,* 226.
[8] S. Mahapatra, H. Koppel, L. S. Cederbaum, *Chem. Phys.* **2000**, *259,* 211.
[9] (a) C. Levy, G. J. Halász, Á. Vibok, I. Bar, Y. Zeiri, R. Kosloff, M. Baer, *J Chem. Phys.* **2008**, *128,* 244302; (b) C. Levy, G. J. Halász, Á. Vibok, I. Bar, Y. Zeiri, R. Kosloff, M. Baer, *J. Phys. Chem. A* **2009**, *113,* 6756.
[10] S. Al-Jabour, M. Baer, O. Deeb, M. Leibscher, J. Manz, X. Xue, S. Zilberg, *J. Phys. Chem. A* **2010**, *114,* 2991.
[11] P. Barragan, L. F. Errea, A. Macias, L. Mendez, A. Riera, J. M. Lucas, A. Aguilar, *J. Chem. Phys.* **2004**, *121,* 11629.
[12] G. J. Halász, Á. Vibók, R. Baer, M. Baer, *J. Chem. Phys.* **2006**, *125,* 094102.
[13] (a) G. J. Halász, Á. Vibók, D. K. Hoffman, D. J. Kouri, M. Baer, *J. Chem. Phys.* **2007**, *126,* 154309; (b) G. J. Halász, Á. Vibók, R. Baer, M. Baer, *J. Phys. A. Math. Theor.* **2007**, *40,* F267; (c) T. Vertesi, R. Englman, *J. Phys. B. At. Mol. Opt. Phys.* **2008**, *41,* 025102; (d) L. Jutier, C. Leonard, F. Gatti, *J. Chem. Phys.* **2000**, *130,* 134301; (e) G. J. Halász, Á. Vibók, *Chem. Phys. Lett.* **2010**, *494,* 150; (f) G. J. Halász, Á. Vibók, *Int. J. Quantum Chem.* **2011**, *111,* 342.
[14] A. Das, D. Mukhopadhyay, S. Adhikari, M. Baer, *J. Chem. Phys.* **2010**, *133,* 084107.
[15] M. Baer, A. Alijah, *Chem. Phys. Lett.* **2000**, *319,* 489.
[16] M. Baer, S. H. Lin, A. Alijah, S. Adhikari, G. D. Billing, *Phys. Rev. A* **2000**, *62,* 032506.
[17] (a) M. V. Berry, *Proc. R. Soc. London. Ser. A* **1984**, *392,* 45; (b) M. Baer, R. Englman, *Mol. Phys.* **1992**, *75,* 283.
[18] (a) T. Ve'rtesi, E. Bene, Á. Vibók, G. J. Halász, M. Baer, *J. Phys. Chem. A* **2005**, *109,* 3476; (b) M. Baer, Beyond Born Oppenheimer; Electronic Non-Adiabatic Coupling Terms and Conical Intersections, Section 8.8.3.2; Wiley: Hoboken, NJ, **2006**.
[19] M. Baer, Beyond Born Oppenheimer; Electronic Non-Adiabatic Coupling Terms and Conical Intersections; Wiley: Hoboken, NJ, **2006**.
[20] (a) M. Baer, *Chem. Phys. Lett.* **1975**, *35,* 112; (b) M. Baer, Beyond Born Oppenheimer; Electronic Non-Adiabatic Coupling Terms and Conical Intersections, Section 5.5.2; Wiley: Hoboken, NJ, **2006**.
[21] M. Baer, A. M. Mebel, G. D. Billing, *Int. J. Quantum Chem.* **2002**, *90,* 1577.
[22] M. Baer, Beyond Born Oppenheimer; Electronic Non-Adiabatic Coupling Terms and Conical Intersections, Section 3.2.2; Wiley: Hoboken, NJ, **2006**.
[23] (a) Z. H. Top, M. Baer, *Chem. Phys.* **1977**, *25,* 1 (see Appendix A); (b) C. Levy, G. J. Halász, Á. Vibok, I. Bar, Y. Zeiri, R. Kosloff, M. Baer, *Int. J. Quantum Chem.* **2009**, *109,* 2482.
[24] K. Stark, H.-J. Werner, *J. Chem. Phys.* **1996**, *104,* 6515.
[25] H. J. Werner, B. Follmeg, M. H. Alexander, *J. Chem. Phys.* **1988**, *89,* 3139.
[26] (a) M. H. Alexander, H.-J. Werner, D. E. Manolopoulos, *J. Chem. Phys.* **1998**, *109,* 5710; (b) M. H. Alexander, D. E. Manolopoulos, H.-J. Werner, *J. Chem. Phys.* **2000**, *113,* 11084.
[27] (a) G. Gaussorgues, C. Le Sech, F. Mosnow-Seeuws, R. McCarrol, A. Riera, *J. Phys. B. At. Mol. Phys.* **1975**, *8,* 239; (b) G. Gaussorgues, C. Le Sech, F. Mosnow-Seeuws, R. McCarrol, A. Riera, *J. Phys. B. At. Mol. Phys.* **1975**, *8,* 253.
[28] (a) M. Born, J. R. Oppenheimer, *Ann. Phys. (Leipzig)* **1927**, *84,* 457; (b) M. Born, *Festschrift. Goett. Nach. Math. Phys.* **1951**, *K1,* 1; (c) M. Born, K. Huang, Dynamical Theory of Crystal Lattices, Chapter IV; Oxford University: New York, **1954**.
[29] A. Yahalom, Advances in Classical Field Theory, Chapter 9; Bentham eBooks, **2011**.
[30] T. G. Heil, S. E. Butler, A. Dalgarno, *Phys. Rev. A* **1981**, *23,* 1100.
[31] V. Sidis, *Adv. Chem. Phys.* **1992**, *82,* 73.
[32] A. Alijah, E. E. Nikitin, *Mol. Phys.* **1999**, *96,* 1399.
[33] M. S. Child, *Adv. Chem. Phys.* **2002**, *124,* 1.
[34] S. Adhikari, G. D. Billing, *Adv. Chem. Phys.* **2002**, *124,* 143.
[35] R. Englman, A. Yahalom, *Adv. Chem. Phys.* **2002**, *124,* 197.
[36] A. Kuppermann, R. Ebrol, *Adv. Chem. Phys.* **2002**, *124,* 283.
[37] (a) R. Baer, *Phys. Rev. Lett.* **2010**, *104,* 073001; (b) I. Ryb, R. Baer, *J. Chem. Phys.* **2004**, *121,* 10370.
[38] E. S. Kryachko, *Adv. Quantum Chem.* **2003**, *44,* 119.
[39] (a) A. J. C. Varandas, B. Sarkar, *Phys. Chem. Chem. Phys.* **2011**, *13,* 8131; (b) B. Sarkar, S. Adhikari, *J. Chem. Phys.* **2006**, *124,* 074101.
[40] (a) C. Hu, O. J. Sugino, K. Watanebe, *Chem. Phys.* **2011**, *135,* 074101; (b) C. Hu, H. Hirai, O. Sugino, *J. Chem. Phys.* **2008**, *128,* 144111.
[41] J. Larson, E. Sjoqvist, *Phys. Rev. A* **2009**, *79,* 043621.
[42] (a) M. S. Kaczmarski, Y. Ma, M. Rohlfing, *Phys. Rev. B* **2010**, *81,* 115433; (b) M. S. Kaczmarski, M. Rohlfing, *J. Phys. B. At. Mol. Phys.* **2010**, *43,* 051001.
[43] T. Van Voorhis, T. Kowalczyk, B. Kaduk, L.-P. Wang, C.-L. Cheng, Q. Wu, *Ann. Rev. Phys. Chem.* **2010**, *61,* 149.
[44] (a) E. Alquire, J. Subotnik, *J. Chem. Phys.* **2011**, *135,* 044114; (b) J. E. Subotmik, S. Yeganeh, R. J. Cave, M. A. Ratner, *J. Chem. Phys.* **2008**, *129,* 244101.
[45] K. Takasuka, T. Yonehara, *Adv. Chem. Phys.* **2010**, *144,* 93.
[46] A. Sirjoosingh, S. Hammes-Schiffer, *J. Phys. Chem. A* **2011**, *115,* 2367.
[47] W. Skomorowski, F. Pawlowski, T. Korona, R. Moszinski, P. S. Zuckowski, J. M. Hutson, *J. Chem. Phys.* **2011**, *134,* 114109.
[48] (a) M. Baer, *Adv. Chem. Phys.* **1982**, *49,* 191 (see p. 283); (b) M. Baer, Beyond Born Oppenheimer; Electronic Non-Adiabatic Coupling Terms and Conical Intersections, Section 3.1.1.3; Wiley: Hoboken, NJ, **2006**.
[49] S. R. Langhoff, E. R. Davidson, *Int. J. Quantum Chem.* **1974**, *8,* 61.

Received: 25 July 2011
Revised: 29 August 2011
Accepted: 30 August 2011
Published online on 29 December 2011